

Persistent Topological Negativity in a High-Temperature Mixed-State

Yonna Kim,¹ Ali Lavasani,² and Sagar Vijay¹

¹*Department of Physics, University of California, Santa Barbara, CA 93106, USA*

²*Kavli Institute for Theoretical Physics, University of California, Santa Barbara, CA, 93106*

We study the entanglement structure of the Greenberger–Horne–Zeilinger (GHZ) state as it thermalizes under a strongly-symmetric quantum channel describing the Metropolis-Hastings dynamics for the d -dimensional classical Ising model at inverse temperature β . This channel outputs the classical Gibbs state when acting on a product state in the computational basis. When applying this channel to a GHZ state in spatial dimension $d > 1$, the resulting mixed state changes character at the Ising phase transition temperature from being long-range entangled to short-range-entangled as temperature increases. Nevertheless, we show that the topological entanglement negativity of a large region is insensitive to this transition and takes the same value as that of the pure GHZ state at any finite temperature $\beta > 0$. We establish this result by devising a local operations and classical communication (LOCC) “decoder” that provides matching lower and upper bounds on the negativity in the thermodynamic limit which may be of independent interest. This perspective connects the negativity to an error-correction problem on the $(d-1)$ -dimensional bipartitioning surface and explains the persistent negativity in certain correlated noise models found in previous studies. Numerical results confirm our analysis.

Introduction: The nature and fate of quantum entanglement in mixed-states of quantum many-body systems – arising in a description of thermal quantum matter or after a pure state experiences local decoherence – have been recently investigated in order to understand the universal quantum correlations that can persist in open quantum systems [1–18]. Patterns of long-range-entanglement (LRE) in mixed quantum matter are intricately related to quantum many-body phases which can act as quantum error-correcting codes [19–21]. Thermal states of quantum many-body systems are also now known to be efficiently classically-preparable at sufficiently high temperatures [22].

The entanglement negativity provides a well-studied diagnostic of bipartite entanglement in a mixed-state, which vanishes if the state can be prepared by from a product state by local operations and classical communication (LOCC) across the entanglement bipartition [23]. While the negativity of a region A grows with the area of its boundary in a generic Gibbs state [24], contributions to the negativity which are independent of coarse-grained details of the bipartitioning surface signal the presence of LRE in a mixed-state and can probe the presence of mixed-state topological quantum order [20]. Diagnostics of non-local mixed-state entanglement, such as the topological entanglement negativity [20], are challenging to study analytically, and the subtle behavior of mixed-state LRE under a finite-depth local quantum channel (FDLC) remains to be fully understood [8, 25].

In this work, we investigate the fate of mixed-state quantum entanglement under a Metropolis-Hastings [26, 27] quantum channel describing the equilibration of a thermal *classical* system, specifically that of a d -dimensional Ising model at inverse temperature β . When acting on a pure state in the computational basis, this channel simply prepares a classical thermal state of the

d -dimensional Ising model.

The nature of the mixed quantum many-body state produced by the action of this channel on a generic input state is more striking. When the initial state is chosen to be a Greenberger–Horne–Zeilinger (GHZ) state, a symmetric, long-range-entangled ground-state of the ferromagnetic phase, we show that the resulting quantum many-body mixed state at any finite temperature $\beta > 0$ has a negativity which is asymptotically exactly that of the pure GHZ state in the limit that the boundary of the sub-region becomes large. In spatial dimensions $d > 1$, the negativity of a large, contiguous region in this mixed state ρ_β is thus *a constant, independent of geometric details of the bipartitioning surface, and insensitive to the thermal phase transition*, as summarized in Eq. (9). Nevertheless, the entanglement properties of the mixed-state do change across this transition; we show that ρ_β cannot be expressed as a convex sum of short-range-entangled (SRE) pure states in the ordered phase but is preparable using an FDLC acting on a product initial state in the high-temperature, disordered phase. This observed behavior is in stark contrast to the negativity of the Gibbs state of a local, quantum many-body Hamiltonian which necessarily vanishes above a finite temperature [22].

This result is established by using the fact that the entanglement negativity is an entanglement monotone [23, 28], so that the negativity of a subregion A of any state ρ , denoted $\mathcal{N}_A(\rho)$, cannot increase under an LOCC operation \mathcal{R} across the bipartitioning surface

$$\mathcal{N}_A(\mathcal{R}[\rho]) \leq \mathcal{N}_A(\rho). \quad (1)$$

This property lends a new perspective on mixed-state negativity, which is of possibly broader interest outside of the specific mixed-states that we study. We explicitly construct an LOCC operation that recovers the GHZ state at any finite temperature and for any bipartition in

the asymptotic limit that the boundary A becomes large. We show that for a contiguous bipartition, this channel is the decoder for a $(d-1)$ -dimensional repetition code, which the two parties in the LOCC protocol must use to determine the precise unitary circuit that must be applied to recover the GHZ state. The well-known success of the $(d-1)$ -dimensional repetition code up to a maximal error strength in dimensions $d > 1$ is intimately related to the recovery of the GHZ state, and thus the constant entanglement negativity, at any finite temperature.

We comment on broader utility of this perspective for understanding mixed-state negativity, by demonstrating that this can provide a simple understanding of why the topological entanglement negativity can remain a constant in correlated noise models (e.g. in [21]).

Setup: Consider N qubits on a d -dimensional hypercubic lattice, in a state described by the density matrix

$$\rho_\beta \equiv \frac{1}{\mathcal{Z}_\beta} \sum_{\sigma} e^{-\beta H} |\psi_\sigma\rangle \langle \psi_\sigma|. \quad (2)$$

Here,

$$H \equiv -J \sum_{\langle i,j \rangle} Z_i Z_j \quad (3)$$

is the energy of a classical Ising model on the d -dimensional hypercubic lattice with ferromagnetic ($J > 0$) nearest-neighbor interactions, while $\mathcal{Z}_\beta \equiv \text{Tr}(e^{-\beta H})$ is the corresponding partition function at inverse temperature β . Furthermore, the state $|\psi_\sigma\rangle \equiv (|\sigma\rangle + U|\sigma\rangle)/\sqrt{2}$, where $|\sigma\rangle \equiv |\sigma_1, \dots, \sigma_N\rangle$ is a product state in the Pauli Z basis, and $U \equiv \prod_j X_j$ is a unitary transformation which generates the Ising symmetry of Eq. (3).

The mixed-state ρ_β is naturally obtained by starting with a GHZ state $|\psi_+\rangle = (|\uparrow \dots \uparrow\rangle + |\downarrow \dots \downarrow\rangle)/\sqrt{2}$, which is an equal-amplitude superposition of the macroscopically-distinct all-up and all-down qubit configurations, and then applying a channel Φ_β which describes a Metropolis-Hastings algorithm [26, 27] in which the energy H is measured, and then a unitary operation X_j is applied on a random qubit with probability $\min\{1, \exp(-\beta \Delta E_j)\}$, where $\Delta E_j \equiv E_{\text{new}} - E_{\text{old}}$ is the energy difference between the new and old qubit configurations.

Repeated measurements and feedback, starting from any product state in the Pauli Z basis, will eventually produce a Gibbs ensemble of the d -dimensional classical Ising model at inverse temperature β [26, 27]. We specifically define Φ_β to be repeated application of the Metropolis-Hastings algorithm so as to produce a thermal steady-state when acting on the all-up state $\rho_0 \equiv |\uparrow \dots \uparrow\rangle \langle \uparrow \dots \uparrow|$, i.e.

$$\Phi_\beta[\rho_0] = \frac{1}{\mathcal{Z}_\beta} \sum_{\sigma} e^{-\beta H} |\sigma\rangle \langle \sigma|. \quad (4)$$

Each operation that comprises the channel Φ_β manifestly commutes with the Ising symmetry transformation U .

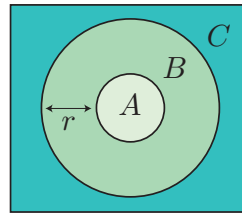


Figure 1: The ABC partitioning used for computing the conditional mutual information $I(A : C | B)$.

Therefore, U is a strong symmetry of this channel [29, 30], i.e. $U\Phi_\beta[\rho] = \Phi_\beta[U\rho]$ for any state ρ , so that

$$\Phi_\beta[|\psi_+\rangle \langle \psi_+|] = \frac{1+U}{\sqrt{2}} \Phi_\beta[\rho_0] \frac{1+U}{\sqrt{2}} = \rho_\beta. \quad (5)$$

Mixed-State Entanglement: The state ρ_β witnesses a thermal phase transition with increasing temperature in spatial dimensions $d > 1$ between a ferromagnetically-ordered and a disordered state. At any temperature, the state ρ_β has a strong Ising symmetry $U\rho_\beta = \rho_\beta$. However, the ferromagnetically-ordered phase is also characterized by long-range-order in local operators which are charged under this symmetry

$\text{Tr}(\rho_\beta Z_i Z_j) \stackrel{|i-j| \rightarrow \infty}{\neq} 0$. These conditions are sufficient to establish [9] that this mixed-state cannot be described as an ensemble of SRE pure-states.

We may also show that in the disordered phase, ρ_β can be prepared by an FDLC, and is thus an SRE mixed-state [31]. In the Supplemental Material [32], we formally show that $\rho_\beta = \mathcal{E}_{ZZ}[|\phi(\beta)\rangle \langle \phi(\beta)|]$, where \mathcal{E}_{ZZ} is a quantum channel that describes maximal dephasing of $Z_i Z_j$ along all nearest-neighbor bonds. Furthermore, we show [32] that the wavefunction $|\phi(\beta)\rangle \equiv \mathcal{Z}_\beta^{-1/2} \sum_{\mu} e^{-\beta H/2} |\mu\rangle$, where $|\mu\rangle$ denotes a product state in the Pauli X basis, is the exact ground-state of the Hamiltonian

$$H_0(\beta) = \sum_j \left[\prod_{i \in \text{NN}(j)} e^{-\beta J Z_i Z_j} - X_j \right], \quad (6)$$

which exhibits a phase transition at a critical value of $\beta = \beta_c(d)$ which is in the d -dimensional Ising universality class. When $\beta < \beta_c(d)$, $|\phi(\beta)\rangle$ is the Ising-symmetric ground-state in the disordered phase and can thus be prepared from a product state using a finite-depth local unitary circuit. Thus in this range of temperatures, ρ_β can be prepared by an FDLC by composing this circuit with the quantum channel \mathcal{E}_{ZZ} .

Conditional Mutual Information: We now investigate entanglement properties of ρ_β and their relation to the Ising phase transition. The conditional mutual information (CMI) is a measure of tripartite correlations in a state and has been used to study various aspects of entanglement in quantum systems[33–38], including prob-

ing mixed state quantum phases of matter[25]. Given subsystems A , B , and C , the CMI is defined as

$$I(A : C|B) = S(AB) + S(BC) - S(B) - S(ABC). \quad (7)$$

Consider the partitioning shown in Fig. 1 with $r > 0$, where C is taken to be the complement of AB . Note that for any proper subset A of qubits, $\rho_{\beta,A} = \text{tr}_{\bar{A}}(\rho_{\beta}) = \rho_{\beta,A}^{\text{Cl}}$, where $\rho_{\beta}^{\text{Cl}} = e^{-\beta H} / \mathcal{Z}_{\beta}$ is the classical Gibbs state [39]. This shows that the first three terms in Eq. (7) take the same value when computed for ρ_{β} as for ρ_{β}^{Cl} . Moreover, it is straightforward to use Eq.(2) to show $S(\rho_{\beta}) = S(\rho_{\beta}^{\text{Cl}}) - \log(2)$. Therefore $I(A : B|C) = \log(2) + I^{\text{Cl}}(A : C|B)$, where $I^{\text{Cl}}(A : C|B)$ is the CMI computed for ρ_{β}^{Cl} . On the other hand, since B is assumed to be non-empty, there is no interaction term in H with support on both A and C and hence $I^{\text{Cl}}(A : C|B) = 0$ [40], and

$$I(A : B|C) = \log(2), \quad (8)$$

independent of r , temperature β and the system size. It is worth mentioning that in contrast, for thermal Gibbs state of local quantum Hamiltonians, CMI decays exponentially with r [41–43].

Entanglement Negativity: We now investigate the entanglement negativity of a subregion A of the mixed-state (2), $\mathcal{N}_A(\rho_{\beta}) \equiv (\|\rho_{\beta}^{T_A}\|_1 - 1)/2$. We will show that for a region A ,

$$\mathcal{N}_A(\rho_{\beta}) = \begin{cases} \frac{1}{2} - O(\exp(-|\partial A|)) & \beta > 0 \\ 0 & \beta = 0 \end{cases} \quad (9)$$

where $|\partial A|$ is the number of qubits on the boundary of A . The second result is easily established. At infinite temperature, $\rho_{\beta=0} = (1 + U)/2^N$, so that $\rho_{\beta=0}^{T_A} = \rho_{\beta=0}$ and $\mathcal{N}_A(\rho_{\beta=0}) = 0$.

The first result is determined as follows. The negativity is a convex function [23, 28] so that

$$\mathcal{N}_A(\rho_{\beta}) \leq \frac{1}{\mathcal{Z}_{\beta}} \sum_{\sigma} e^{\beta J \sum_{\langle i,j \rangle} \sigma_i \sigma_j} \mathcal{N}_A(|\psi_{\sigma}\rangle\langle\psi_{\sigma}|) = \frac{1}{2} \quad (10)$$

for any region A , since $|\psi_{\sigma}\rangle$ is related to the GHZ state $|\psi_{+}\rangle$ by single qubit gates, so that $\mathcal{N}_A(|\psi_{\sigma}\rangle\langle\psi_{\sigma}|) = \mathcal{N}_A(|\psi_{+}\rangle\langle\psi_{+}|)$. The latter is exactly 1/2 for any region A . The negativity is also an entanglement monotone [23, 28], see Eq. (1). Here, we show that given the state ρ_{β} for any $\beta > 0$ and any region A , there is an LOCC operation \mathcal{R} with respect to A and its complement \bar{A} that recovers the GHZ state with a fidelity that approaches unity exponentially quickly in the size of the boundary of A . Combining this with (10), allows us to establish Eq. (9).

We first construct the LOCC channel \mathcal{R} for a contiguous bipartition, before generalizing this construction for a non-contiguous subregion A . The state ρ_{β} describes the ensemble of pure-states $|\psi_{\sigma}\rangle$ drawn with probability

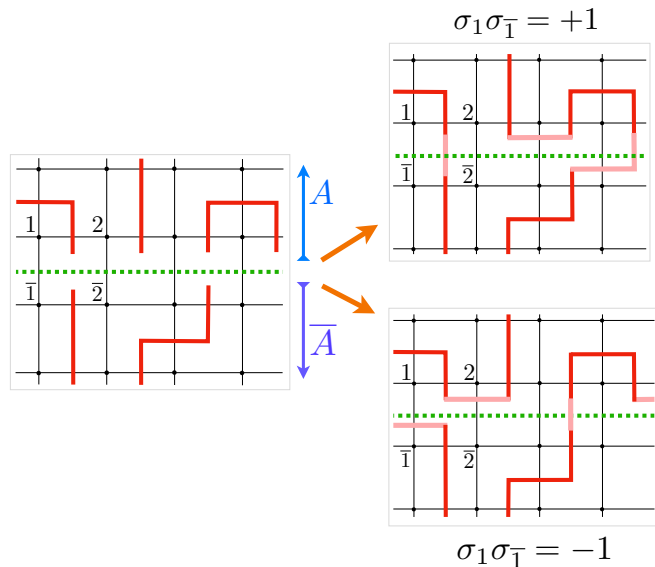


Figure 2: Measurements of domain walls that lie exclusively within A or \bar{A} lead to configurations such as the one shown in the left panel, with domain walls indicated by red lines on the dual lattice. There are two possibilities for how these domain wall connect across this interface, corresponding the choice $\sigma_1 \sigma_{\bar{1}} = \pm 1$.

$e^{\beta J \sum_{\langle i,j \rangle} \sigma_i \sigma_j} / \mathcal{Z}_{\beta}$. Given a state from this ensemble, we measure the operators $Z_i Z_j$ along all nearest-neighbor bonds lying exclusively within A or \bar{A} . The resulting pattern of domain walls – an example of which is shown in the left panel of Fig. 2 in two spatial dimensions – is consistent with having drawn the state $|\psi_{\sigma}\rangle$ or the state $\prod_{j \in A} X_j |\psi_{\sigma}\rangle$ and thus leaves one classical bit’s worth of ambiguity in determining the precise state. Equivalently, this ambiguity corresponds to the two possible ways that the observed domain walls can connect across the bipartition, as shown in Fig. 2.

The preparation of the GHZ state through LOCC thus maps onto a decoding problem in a classical $(d - 1)$ -dimensional repetition code living on the interface between A and \bar{A} . The classical bit of information is the relative alignment of any two qubits across the bipartition in the Pauli Z basis (e.g. in Fig. 2, the classical bit can be taken to be $\tau_1 \equiv \sigma_1 \sigma_{\bar{1}}$). The measured “syndromes” of the repetition code (e.g. $\tau_1 \tau_2 = (\sigma_1 \sigma_2)(\sigma_{\bar{1}} \sigma_{\bar{2}})$) and the Boltzmann weights for the d -dimensional Ising model are used to perform maximum-likelihood decoding to guess the correct state. Specifically, let w_1 and w_2 denote the Boltzmann weights corresponding to states (i) $|\psi_{\sigma}\rangle$ and (ii) $\prod_{j \in A} X_j |\psi_{\sigma}\rangle$, respectively. We will guess that the state we have is (i) with probability $p \equiv w_1 / (w_1 + w_2)$ and (ii) with probability $1 - p$. We will subsequently apply the appropriate single-site unitary gates to turn this into the GHZ state. The LOCC channel is thus

1. Measure $Z_i Z_j$ along all nearest-neighbor bonds ly-

ing exclusively within A or \bar{A} .

- Let $|\sigma\rangle$ be a product state in the Pauli Z basis which is consistent with the measurement outcomes. Apply the unitary $U_1 = \prod_j X_j^{(1-\sigma_j)/2}$ with probability p , or the unitary $U_2 = \prod_{j \in A} X_j \prod_j X_j^{(1-\sigma_j)/2}$ with probability $1-p$.

At any finite temperature, the relative probability $p/(1-p) = w_1/w_2$ scales exponentially in the size of the boundary of A , due to the fact that the energy of an Ising domain wall is extensive in its length. Thus, the decoder for the repetition code should be successful at any finite temperature, and fail exactly at infinite temperature when $w_1 = w_2 = 1/2$. This is consistent with the known behavior of the repetition code with single-qubit bit-flip errors with probability q , for which perfect decoding is possible for any $q \leq 1/2$.

We may generalize this channel for the case where A is a non-contiguous region. In this case, step 1 (above) is replaced by measurements of $Z_i Z_j$ across *all* pairs of sites entirely within A and entirely within \bar{A} . As before, only one classical bit's worth of ambiguity thus remains after these measurements, in determining the precise state. The quantum circuit that takes this state onto the GHZ state is then determined by a decoder for a repetition code with $|\partial A|$ sites. Thus, decoding the correct quantum circuit should again be successful at any $\beta > 0$, as $|\partial A|$ becomes large, regardless of the geometry of the bipartition.

Consistent with these expectations, we show [32] that for any bipartition, the fidelity of the recovered state $R(\rho_\beta)$ with the GHZ state is exactly

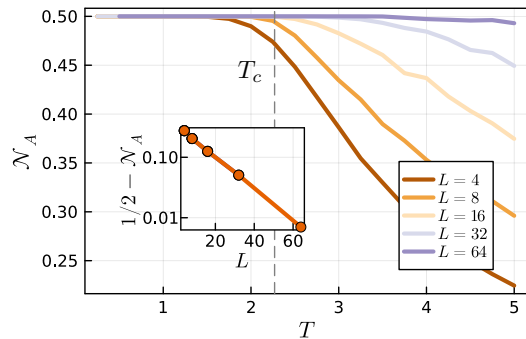
$$\mathcal{F}(R(\rho_\beta), |\psi_+\rangle \langle \psi_+|) = \frac{1}{2} \left[1 - \langle \tanh(\beta H_\partial) \rangle \right] \quad (11)$$

where H_∂ denotes terms in the Ising Hamiltonian acting exclusively along bonds that cross the bipartition between A and \bar{A} and the expectation value is taken in the thermal state for the classical Ising model. At any finite temperature, the energy H_∂ is negative, and extensively large in the boundary of A , so that $\langle \tanh(\beta H_\partial) \rangle \rightarrow 1$ as A becomes large.

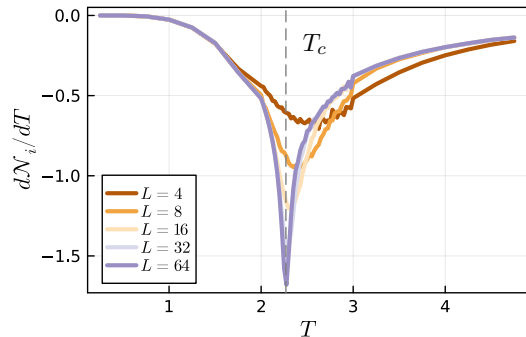
Numerical Results: To numerically confirm this result, we obtain an alternate expression for the entanglement negativity of any bi-partition [32]

$$\mathcal{N}_A[\rho_\beta] = \frac{1}{4} \left\langle \left| 1 - e^{2\beta H_\partial[\sigma]} \right| \right\rangle. \quad (12)$$

One may now use classical Monte Carlo simulations to compute the thermal average in Eq.(12). However, care must be taken with sampling the spin configurations, since the expression inside the absolute value could be exponentially large for configurations with an exponentially small Boltzmann weight, in such a way that the overall contribution to the expectation value is $O(1)$.



(a)



(b)

Figure 3: a) Entanglement Negativity \mathcal{N}_A versus temperature in the state ρ_β in $d = 2$, where subregion A is taken to be half the system. The inset shows $1/2 - \mathcal{N}_A$ at $T = 5$ versus L in a semi-log plot, which shows that \mathcal{N}_A saturates exponentially quickly in the size of the boundary. b) Derivative of entanglement negativity of a single site with respect to temperature, showing a singularity at the Ising phase transition temperature.

The aforementioned issue can be avoided by using a technique known as importance sampling. Let $q[\sigma]$ denote the probability distribution defined as $q[\sigma_A, \sigma_{\bar{A}}] = \frac{1}{2}p[\sigma_A, \sigma_{\bar{A}}] + \frac{1}{2}p[\sigma_A, \bar{\sigma}_{\bar{A}}]$, where $p[\sigma] = e^{\beta J \sum_{\langle i,j \rangle} \sigma_i \sigma_j} / \mathcal{Z}_\beta$. To sample from $q[\sigma]$, one can simply sample from $p[\sigma]$ and then with $1/2$ probability, flip the spins in \bar{A} . We may thus write Eq.(12) as,

$$\begin{aligned} \mathcal{N}_A[\rho_\beta] &= \frac{1}{4} \sum_{\sigma} q[\sigma] \frac{p[\sigma]}{q[\sigma]} |1 - e^{2\beta H_\partial[\sigma]}| \\ &= \frac{1}{2} \langle |\tanh(\beta H_\partial[\sigma])| \rangle_q. \end{aligned} \quad (13)$$

where the final expectation value is taken with respect to the distribution q . The advantage of Eq.(13) compared to Eq.(12) is that the expression inside the expectation value is now bounded by unity everywhere, so that contributions from rare configurations are no longer a concern.

In the following we present the numerical results for a

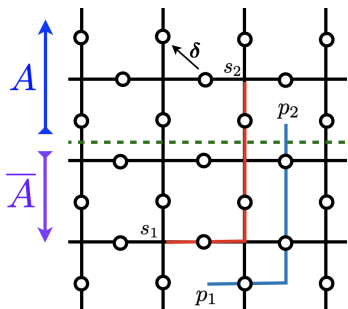


Figure 4: Dephasing of the toric code by the local operators $Z_{j+\delta}X_j$ at each lattice site j as studied in Ref. [21]. Correlations in the syndromes permit perfect preparation of a mixed-state within the ground-space of the toric code using LOCC across A and \bar{A} .

2D system of qubits placed on a $L \times L$ square lattice with periodic boundary conditions. Fig. 3a shows the negativity $\mathcal{N}_A(\rho_\beta)$ when A is taken to be the $L \times \frac{L}{2}$ cylinder. As is clear from Fig. 3a, in the thermodynamic limit, the negativity is equal to $1/2$ even above the Ising critical temperature (marked by the dashed line in Fig. 3a), as expected from the expression in (13). The fact that the negativity of subregions with extensive boundary is $1/2$ irrespective of temperature, means that if one defines the topological negativity as the constant contribution to the negativity as in Ref. [2], one would find that the resulting mixed state has $\mathcal{N}_{\text{topo}} = -1/2$ even above the critical temperature, despite the fact that for $T > T_c$ – as shown above – ρ_β is an SRE mixed-state. [5, 6, 44–46] (cf. Ref. [20]).

Although the thermal phase transition at T_c has no effect in the negativity of subregions with extensive boundaries, the negativity of finite subregions (while continuous) becomes singular at $T = T_c$. Fig. 3b shows the derivative of the negativity of a single site with respect to temperature which shows a singularity at $T = T_c$, which is consistent with the singularity of the heat capacity at the $d = 2$ classical Ising phase transition, as to be expected from Eq. (12).

Discussion and Outlook: Using LOCC to recover states with a known pattern of LRE may provide another perspective that can be used to investigate mixed-state LRE under decoherence. For correlated decoherence, this is apparent in specific examples. The two-dimensional toric code dephased by local operators $Z_{j+\delta}X_j$ at each site j , with the vector δ given in Fig. 4, was studied in Ref. [21]. Quantum state trajectories under this channel only contain patterns of \mathbb{Z}_2 charge and flux which are separated by δ . Therefore, for any dephasing strength, it is possible to use LOCC across the bipartition in Fig. 4 to deterministically recover the toric code ground-state. The \mathbb{Z}_2 charge and flux lying on the bipartitioning surface, which cannot be directly measured in the LOCC protocol, can be perfectly inferred from stabilizer mea-

surements in A and \bar{A} due to the noise correlations. The negativity for this bipartition and for any dephasing strength [21] is thus *exactly* that of the toric-code ground-state [47]. Another example for which the LOCC perspective presented here could be insightful is the study of entanglement structure in the toric code with single-site Y decoherence [48, 49]. In this case, while the noise model itself is not correlated, the LOCC protocol can benefit from the correlations that are present in the syndromes due to the extensively many strong symmetries of this channel [48, 50]. The detailed study of this model and other correlated noise models is left to a future work.

We identify other directions implied by our results. First, it is interesting to consider the fate of mixed-state entanglement under thermalization by genuinely quantum channels which are strongly-symmetric. More concretely, we may consider thermalizing the GHZ state via a strongly symmetric implementation of the *quantum* Metropolis-Hastings dynamics [51, 52] for the d -dimensional transverse field quantum Ising model. The resulting mixed state would be the projection of the quantum Gibbs state onto the symmetric sector. A similar LOCC protocol to recover the GHZ state can be used to relate the entanglement negativity to the performance of a $(d-1)$ -dimensional repetition code under a *coherent* correlated noise model. Energetic considerations can be used to argue about the success of the LOCC protocol in turning the resulting mixed state into the GHZ state. This lower bounds the negativity of the resulting mixed-state and may suggest that it would have a non-trivial negativity at high temperatures, though this remains to be confirmed.

Second, while the persistence of topological negativity at high temperatures in our work can be understood as a consequence of the repetition code possessing maximum error threshold, it is interesting to search for settings where a similar line of argument would lead to a different code with a finite threshold. Such a system, would exhibit a finite temperature phase transition in negativity, which may not necessarily coincide with the standard order-disorder thermal phase transition. Furthermore, while we focused on the Metropolis-Hastings channel for the classical Ising model, a possibly fruitful future direction to pursue is to consider other classical systems with different symmetries and study the fate of entanglement in an initially symmetric state (e.g. continues symmetries, higher-form symmetries or non-Abelian symmetries [53, 54]).

Lastly, given that the topological negativity is unable to detect the phase transition in the complexity of the mixed-state ρ_β (from LRE to SRE), it is interesting to look for other quantities that would be able to capture the complexity of the quantum phase transition in our system as well as in more general settings.

Acknowledgments: We thank Yimu Bao, Matthew Fisher, Tarun Grover, Tibor Rakovszky, Subhayan Sahu,

Shengqi Sang and Yaodong Li for useful discussions. This research was supported in part by grant NSF PHY-2309135 to the Kavli Institute for Theoretical Physics (KITP). Use was made of computational facilities purchased with funds from the National Science Foundation (CNS-1725797) and administered by the Center for Scientific Computing (CSC). The CSC is supported by the California NanoSystems Institute and the Materials Research Science and Engineering Center (MRSEC; NSF DMR 2308708) at UC Santa Barbara. SV is partly supported as an Alfred P. Sloan Research Fellow.

-
- [1] K.-H. Wu, T.-C. Lu, C.-M. Chung, Y.-J. Kao, and T. Grover, Entanglement renyi negativity across a finite temperature transition: a monte carlo study, *Physical Review Letters* **125**, 140603 (2020).
- [2] T.-C. Lu and T. Grover, Structure of quantum entanglement at a finite temperature critical point, *Physical Review Research* **2**, 043345 (2020).
- [3] T.-C. Lu and S. Vijay, Characterizing long-range entanglement in a mixed state through an emergent order on the entangling surface, *Physical Review Research* **5**, 033031 (2023).
- [4] R. Fan, Y. Bao, E. Altman, and A. Vishwanath, Diagnostics of mixed-state topological order and breakdown of quantum memory, *PRX Quantum* **5**, 020343 (2024).
- [5] Y.-H. Chen and T. Grover, Symmetry-enforced many-body separability transitions, arXiv preprint arXiv:2310.07286 (2023).
- [6] Y.-H. Chen and T. Grover, Separability transitions in topological states induced by local decoherence, *Physical Review Letters* **132**, 170602 (2024).
- [7] Y.-H. Chen and T. Grover, Unconventional topological mixed-state transition and critical phase induced by self-dual coherent errors, arXiv preprint arXiv:2403.06553 (2024).
- [8] S. Sang, Y. Zou, and T. H. Hsieh, Mixed-state quantum phases: Renormalization and quantum error correction, arXiv preprint arXiv:2310.08639 (2023).
- [9] T.-C. Lu, Z. Zhang, S. Vijay, and T. H. Hsieh, Mixed-state long-range order and criticality from measurement and feedback, *PRX Quantum* **4**, 030318 (2023).
- [10] L. A. Lessa, M. Cheng, and C. Wang, Mixed-state quantum anomaly and multipartite entanglement, arXiv preprint arXiv:2401.17357 (2024).
- [11] Z. Zhang, U. Agrawal, and S. Vijay, Quantum communication and mixed-state order in decohered symmetry-protected topological states, arXiv preprint arXiv:2405.05965 (2024).
- [12] J. Y. Lee, C.-M. Jian, and C. Xu, Quantum criticality under decoherence or weak measurement, *PRX quantum* **4**, 030317 (2023).
- [13] C. de Groot, A. Turzillo, and N. Schuch, Symmetry protected topological order in open quantum systems, *Quantum* **6**, 856 (2022).
- [14] G.-Y. Zhu, N. Tantivasadakarn, A. Vishwanath, S. Trebst, and R. Verresen, Nishimori's cat: stable long-range entanglement from finite-depth unitaries and weak measurements, *Physical Review Letters* **131**, 200201 (2023).
- [15] J. Y. Lee, Y.-Z. You, and C. Xu, Symmetry protected topological phases under decoherence, arXiv preprint arXiv:2210.16323 (2022).
- [16] Z. Wang, X.-D. Dai, H.-R. Wang, and Z. Wang, Topologically ordered steady states in open quantum systems, arXiv preprint arXiv:2306.12482 (2023).
- [17] Z. Wang and L. Li, Anomaly in open quantum systems and its implications on mixed-state quantum phases, arXiv preprint arXiv:2403.14533 (2024).
- [18] J. Y. Lee, W. Ji, Z. Bi, and M. Fisher, Decoding measurement-prepared quantum phases and transitions: from ising model to gauge theory, and beyond, arXiv preprint arXiv:2208.11699 (2022).
- [19] Y. Bao, R. Fan, A. Vishwanath, and E. Altman, Mixed-state topological order and the errorfield double formulation of decoherence-induced transitions, arXiv preprint arXiv:2301.05687 (2023).
- [20] T.-C. Lu, T. H. Hsieh, and T. Grover, Detecting topological order at finite temperature using entanglement negativity, *Physical Review Letters* **125**, 116801 (2020).
- [21] Z. Wang, Z. Wu, and Z. Wang, Intrinsic mixed-state topological order without quantum memory, arXiv preprint arXiv:2307.13758 (2023).
- [22] A. Bakshi, A. Liu, A. Moitra, and E. Tang, High-temperature gibbs states are unentangled and efficiently preparable, arXiv preprint arXiv:2403.16850 (2024).
- [23] G. Vidal and R. F. Werner, Computable measure of entanglement, *Physical Review A* **65**, 032314 (2002).
- [24] N. E. Sherman, T. Devakul, M. B. Hastings, and R. R. Singh, Nonzero-temperature entanglement negativity of quantum spin models: Area law, linked cluster expansions, and sudden death, *Physical Review E* **93**, 022128 (2016).
- [25] S. Sang and T. H. Hsieh, Stability of mixed-state quantum phases via finite markov length, arXiv preprint arXiv:2404.07251 (2024).
- [26] N. Metropolis, A. W. Rosenbluth, M. N. Rosenbluth, A. H. Teller, and E. Teller, Equation of state calculations by fast computing machines, *The journal of chemical physics* **21**, 1087 (1953).
- [27] W. K. Hastings, Monte carlo sampling methods using markov chains and their applications, (1970).
- [28] M. B. Plenio, Logarithmic negativity: a full entanglement monotone that is not convex, *Physical review letters* **95**, 090503 (2005).
- [29] V. V. Albert and L. Jiang, Symmetries and conserved quantities in lindblad master equations, *Physical Review A* **89**, 022118 (2014).
- [30] S. Lieu, R. Belyansky, J. T. Young, R. Lundgren, V. V. Albert, and A. V. Gorshkov, Symmetry breaking and error correction in open quantum systems, *Physical Review Letters* **125**, 240405 (2020).
- [31] The ability to prepare ρ_β by an FDLC implies that this mixed-state describes an ensemble of SRE pure state.
- [32] See supplemental material.
- [33] M. Levin and X.-G. Wen, Detecting topological order in a ground state wave function, *Physical review letters* **96**, 110405 (2006).
- [34] K. Kato, F. Furrer, and M. Muraio, Information-theoretical analysis of topological entanglement entropy and multipartite correlations, *Physical Review A* **93**, 022317 (2016).
- [35] D. Ding, P. Hayden, and M. Walter, Conditional mutual

- information of bipartite unitaries and scrambling, *Journal of High Energy Physics* **2016**, 1 (2016).
- [36] O. Fawzi and R. Renner, Quantum conditional mutual information and approximate markov chains, *Communications in Mathematical Physics* **340**, 575 (2015).
- [37] S.-u. Lee, C. Oh, Y. Wong, S. Chen, and L. Jiang, Universal spreading of conditional mutual information in noisy random circuits, arXiv preprint arXiv:2402.18548 (2024).
- [38] Y. Zhang and S. Gopalakrishnan, Nonlocal growth of quantum conditional mutual information under decoherence, arXiv preprint arXiv:2402.03439 (2024).
- [39] This in particular shows that for mutual information we have $I(A : C) = I^{\text{Cl}}(A : C)$ provided that $r > 0$, where I^{Cl} is computed with respect to ρ_{β}^{Cl} .
- [40] P. Clifford and J. Hammersley, Markov fields on finite graphs and lattices, (1971).
- [41] K. Kato and F. G. Brandao, Quantum approximate markov chains are thermal, *Communications in Mathematical Physics* **370**, 117 (2019).
- [42] T. Kuwahara, K. Kato, and F. G. Brandão, Clustering of conditional mutual information for quantum gibbs states above a threshold temperature, *Physical review letters* **124**, 220601 (2020).
- [43] T. Kuwahara, Clustering of conditional mutual information and quantum markov structure at arbitrary temperatures, arXiv preprint arXiv:2407.05835 (2024).
- [44] R. F. Werner, Quantum states with einstein-podolsky-rosen correlations admitting a hidden-variable model, *Physical Review A* **40**, 4277 (1989).
- [45] M. B. Hastings, Topological order at nonzero temperature, *Physical review letters* **107**, 210501 (2011).
- [46] R. Ma and C. Wang, Average symmetry-protected topological phases, *Physical Review X* **13**, 031016 (2023).
- [47] C. Castelnuovo, Negativity and topological order in the toric code, *Physical Review A—Atomic, Molecular, and Optical Physics* **88**, 042319 (2013).
- [48] D. K. Tuckett, A. S. Darmawan, C. T. Chubb, S. Bravyi, S. D. Bartlett, and S. T. Flammia, Tailoring surface codes for highly biased noise, *Physical Review X* **9**, 041031 (2019).
- [49] T. Ellison and M. Cheng, Towards a classification of mixed-state topological orders in two dimensions, arXiv preprint arXiv:2405.02390 (2024).
- [50] J. Hauser, Y. Bao, S. Sang, A. Lavasani, U. Agrawal, and M. Fisher, Information dynamics in decohered quantum memory with repeated syndrome measurements: a dual approach, arXiv preprint arXiv:2407.07882 (2024).
- [51] K. Temme, T. J. Osborne, K. G. Vollbrecht, D. Poulin, and F. Verstraete, Quantum metropolis sampling, *Nature* **471**, 87 (2011).
- [52] M.-H. Yung and A. Aspuru-Guzik, A quantum–quantum metropolis algorithm, *Proceedings of the National Academy of Sciences* **109**, 754 (2012).
- [53] Y. Li, F. Pollmann, N. Read, and P. Sala, Highly-entangled stationary states from strong symmetries, arXiv preprint arXiv:2406.08567 (2024).
- [54] A. Moharramipour, L. A. Lessa, C. Wang, T. H. Hsieh, and S. Sahu, Symmetry enforced entanglement in maximally mixed states, arXiv preprint arXiv:2406.08542 (2024).
- [55] Another way to derive this pre-factor is to observe that for a given configuration of μ_j satisfying the constraint $\prod_j \mu_j = 1$, there are $2^{N_b}/2^{N-1}$ different configurations of σ_{ij} such that $\mu_j = A_j[\sigma]$.
- [56] T. Cacoullos, *Exercises in probability* (Springer Science & Business Media, 2012).

Supplemental Material

Entanglement of ρ_β

Here, we show that the state (2) is short-range-entangled (SRE) throughout the disordered phase at sufficiently high temperatures, and in any spatial dimension. First, observe that this state may be written as

$$\rho_\beta = \sum_{\mu} p_{\mu} |\phi_{\mu}\rangle \langle \phi_{\mu}| \quad (14)$$

where $|\phi_{\mu}\rangle \equiv \rho_{\beta}^{1/2} |\mu\rangle / \sqrt{p_{\mu}}$ and $p_{\mu} \equiv \langle \mu | \rho_{\beta} | \mu \rangle$, while $|\mu\rangle$ is a product state in the Pauli X basis. Because of the strong symmetry of this state, $\text{Tr}(\rho_{\beta} U) = 1$, where $U \equiv \prod_j X_j$. As a result, each pure state appearing in (14) must satisfy $\prod_j X_j |\phi_{\mu}\rangle = |\phi_{\mu}\rangle$.

Furthermore, observe that

$$\rho_{\beta}^{1/2} = \frac{1}{\sqrt{\mathcal{Z}_{\beta}}} \sum_{\sigma} e^{-\beta H/2} |\psi_{\sigma}\rangle \langle \psi_{\sigma}| \quad (15)$$

It is evident from this expression that $[Z_i Z_j, \rho_{\beta}^{1/2}] = 0$ for any i, j . As a result, any state $|\phi_{\mu}\rangle$ appearing in (14) – for which $U |\phi_{\mu}\rangle = |\phi_{\mu}\rangle$ – can be obtained by applying single-site unitary gates on the reference state $|\phi_{+}\rangle = \rho_{\beta}^{1/2} |+\cdots+\rangle / \sqrt{p_{+}}$, where $|+\cdots+\rangle$ is a product state in which $X_j = +1$ for each qubit:

$$|\phi_{\mu}\rangle = \prod_j Z_j^{\frac{1-\mu_j}{2}} |\phi_{+}\rangle \quad (16)$$

Finally, we note that $p_{\mu} = \langle \mu | \rho_{\beta} | \mu \rangle = \langle +\cdots+ | \prod_j Z_j^{\frac{1-\mu_j}{2}} \rho_{\beta} \prod_j Z_j^{\frac{1-\mu_j}{2}} | +\cdots+ \rangle = \langle +\cdots+ | \rho_{\beta} | +\cdots+ \rangle = p_{+}$. As a result, $p_{\mu} = 1/2^{N-1}$ where N is the total number of qubits. To summarize, we may write (14) as

$$\rho_{\beta} = \frac{1}{2^{N-1}} \sum_{\mu \text{ s.t. } \prod_j \mu_j = +1} \prod_j Z_j^{\frac{1-\mu_j}{2}} |\phi_{+}\rangle \langle \phi_{+}| \prod_j Z_j^{\frac{1-\mu_j}{2}} \quad (17)$$

We now re-cast the summation by introducing Ising degrees of freedom σ_{ij} along bonds of the hypercubic lattice, and letting $\mu_j \equiv A_j[\sigma] \equiv \prod_{i \in \text{NN}(j)} \sigma_{ij}$, where the product is taken over sites that are nearest-neighbor to j . With periodic boundary conditions, $\prod_j A_j[\sigma] = +1$, and as a result, the constraint on the summation $\prod_j \mu_j = +1$ is naturally satisfied by this replacement. With this replacement, we may write

$$\rho_{\beta} = \frac{1}{2^{N_b}} \sum_{\sigma} \prod_j Z_j^{\frac{1-A_j[\sigma]}{2}} |\phi_{+}\rangle \langle \phi_{+}| \prod_j Z_j^{\frac{1-A_j[\sigma]}{2}} \quad (18)$$

Here, $N_b = d \cdot N$ is the total number of bonds on the d -dimensional hypercubic lattice. The pre-factor ensures the normalization of the density matrix[55]. Finally, using the fact that $Z_j^{\frac{1-A_j[\sigma]}{2}} = \prod_{i \in \text{NN}(j)} Z_j^{\frac{1-\sigma_{ij}}{2}}$, we may write $\prod_j Z_j^{\frac{1-A_j[\sigma]}{2}} = \prod_{\langle i,j \rangle} (Z_i Z_j)^{\frac{1-\sigma_{ij}}{2}}$, where the product in the second expression is taken over distinct, nearest-neighbor bonds. As a result,

$$\rho_{\beta} = \frac{1}{2^{N_b}} \sum_{\sigma} \prod_{\langle i,j \rangle} (Z_i Z_j)^{\frac{1-\sigma_{ij}}{2}} |\phi_{+}\rangle \langle \phi_{+}| \prod_{\langle i,j \rangle} (Z_i Z_j)^{\frac{1-\sigma_{ij}}{2}} \quad (19)$$

We conclude that ρ_{β} may be obtained by dephasing $Z_i Z_j$ on each bond of the lattice, with *maximal* strength, a manifestly finite-depth, local quantum channel.

Finally, we may argue that the state $|\phi_{+}\rangle$ is SRE when the system is in a disordered phase. We do this by first writing

$$|\phi_{+}\rangle = \sqrt{2^{N-1}} \rho_{\beta}^{1/2} |+\cdots+\rangle = \sqrt{\frac{2^{N-1}}{\mathcal{Z}_{\beta}}} \sum_{\sigma} e^{-\beta H/2} |\psi_{\sigma}\rangle \langle \psi_{\sigma}| |+\cdots+\rangle = \frac{1}{\sqrt{\mathcal{Z}_{\beta}}} \sum_{\sigma} e^{-\beta H/2} |\sigma\rangle \quad (20)$$

We now observe that (20) is the ground-state of the Hamiltonian

$$H = - \sum_j Q_j \quad (21)$$

where

$$Q_j \equiv -X_j + \prod_{i \in \text{NN}(j)} e^{-\beta J Z_i Z_j} \quad (22)$$

LOCC Operations and Recovering the GHZ State

Here, we will show the existence of an LOCC protocol \mathcal{R} with respect to bi-partition A and \bar{A} , which transforms state ρ_β back to the GHZ state in the thermodynamic limit. The LOCC protocol consists of two steps:

1. Measure $Z_i Z_j$ on each link that is entirely in A or in \bar{A} subregions, finding the outcome $\mu_{ij} = \pm 1$. This does **not** include the links across the boundary, ∂A .
2. For any given set of measurement outcomes $\mu = \{\mu_{i,j}\}$, there exist two possible states which have domain wall configuration consistent with μ . We pick one of the two states based on a coin toss weighted with their respective Boltzmann weight in ρ_β (Eq.(2)) and apply a product of Pauli X_i operators to eliminate the domain walls in that assumed configuration.

In the following, we will derive Eq.(11) for the fidelity between the GHZ state, $|\psi_+\rangle$, and the output state $\mathcal{R}(\rho_\beta)$.

Fidelity

Let $\{M_\mu\}$ be the projective measurements that measure whether there is a domain wall or not on the links which are entirely in region A or \bar{A} ,

$$M_\mu \equiv \prod_{\langle i,j \rangle \in A, \bar{A}} \frac{1 + \mu_{i,j} Z_i Z_j}{2}, \quad (23)$$

where μ_{ij} is the measurement outcome of measuring $Z_i Z_j$ and the product only includes next nearest sites which are both in A or both in \bar{A} . Note that,

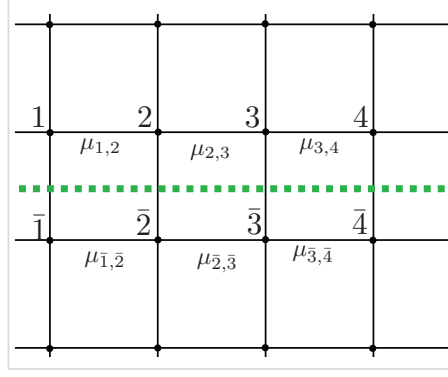
$$M_\mu |\psi_\sigma\rangle = \prod_{\langle i,j \rangle \in A, \bar{A}} \delta_{\mu_{i,j}, \sigma_i \sigma_j} |\psi_\sigma\rangle. \quad (24)$$

A set of measurement outcomes μ specifies a certain domain wall configuration in A and \bar{A} , with some domain walls ending on the boundary ∂A . Let $1 \in A$ and $\bar{1} \in \bar{A}$ be two adjacent sites across the boundary and define $\tau = \pm 1$ to be a marker for whether or not there is a domain wall across the edge connecting 1 and $\bar{1}$, i.e. $\tau \equiv \sigma_1 \sigma_{\bar{1}}$ (see Fig. 2). Note that μ and τ together uniquely specify the global domain wall configuration, because there should be even number of domain walls across each plaquette of the square lattice. In particular if we label the sites along the boundary as shown in Fig.5, we have,

$$\sigma_i \sigma_{\bar{i}} = \tau \prod_{j=1}^{i-1} \mu_{j,j+1} \mu_{\bar{j},\bar{j}+1}. \quad (25)$$

Let $X_{\mu,\tau}$ be the appropriate product of single qubit Pauli- X s that corresponds to the domain wall configuration specified by μ and τ . In particular, if $M_\mu |\psi_\sigma\rangle = |\psi_\sigma\rangle$, we have

$$X_{\mu,\tau} |\psi_\sigma\rangle \equiv \begin{cases} |\psi_+\rangle & \text{if } \sigma_1 \sigma_{\bar{1}} = \tau \\ \prod_{j \in A} X_j |\psi_+\rangle & \text{if } \sigma_1 \sigma_{\bar{1}} \neq \tau. \end{cases} \quad (26)$$

Figure 5: Labeling the boundary sites in A and \bar{A}

Given the measurement outcomes μ , the decoder \mathcal{R} applies $X_{\mu,\tau}$ with $\tau = \pm 1$ chosen randomly with probability $P_{\mu,\tau}$. The probability $P_{\mu,\tau}$ is chosen to be proportional to the Boltzmann weight of the spin configuration specified by μ and τ and according to Eq.(25) can be written as,

$$P_{\mu,\tau} = \frac{e^{\beta J \tau \sum_{i \geq 1} \prod_{j=1}^{i-1} \mu_{j,j+1} \mu_{\bar{j},\bar{j}+1}}}{\sum_{\tau'=\pm 1} e^{\beta J \tau' \sum_{i \geq 1} \prod_{j=1}^{i-1} \mu_{j,j+1} \mu_{\bar{j},\bar{j}+1}}}. \quad (27)$$

Putting everything together, we can compute the average “decoding” fidelity,

$$F = \langle \psi_+ | \mathcal{R}(\rho_\beta) | \psi_+ \rangle = \sum_{\sigma,\mu,\tau} \frac{e^{-\beta H[\sigma]}}{\mathcal{Z}_\beta} P_{\mu,\tau} |\langle \psi_+ | X_{\mu,\tau} M_\mu | \psi_\sigma \rangle|^2. \quad (28)$$

Using Eqs.(24) and (26) this simplifies to

$$F = \sum_{\sigma,\mu,\tau} \frac{e^{-\beta H[\sigma]}}{\mathcal{Z}_\beta} P_{\mu,\tau} \prod_{\langle i,j \rangle \in A, \bar{A}} \delta_{\mu_{i,j}, \sigma_i \sigma_j} \delta_{\sigma_1 \sigma_{\bar{1}}, \tau}. \quad (29)$$

Plugging the expression for $P_{\mu,\tau}$ into Eq. (29), we get

$$F = \sum_{\sigma,\tau} \frac{e^{-\beta H[\sigma]}}{\mathcal{Z}_\beta} \frac{e^{\beta J \tau \sum_{i \geq 1} \sigma_1 \sigma_i \sigma_{\bar{1}} \sigma_{\bar{i}}}}{\sum_{\tau'=\pm 1} e^{\beta J \tau' \sum_{i \geq 1} \sigma_1 \sigma_i \sigma_{\bar{1}} \sigma_{\bar{i}}}} \delta_{\sigma_1 \sigma_{\bar{1}}, \tau} \quad (30)$$

$$= \sum_{\sigma} \frac{e^{-\beta H[\sigma]}}{\mathcal{Z}_\beta} \frac{e^{\beta J \sum_{i \geq 1} \sigma_i \sigma_{\bar{i}}}}{\sum_{\tau'=\pm 1} e^{\beta \tau' \sigma_1 \sigma_{\bar{1}} J \sum_{i \geq 1} \sigma_i \sigma_{\bar{i}}}} \quad (31)$$

$$= \frac{1}{2} \sum_{\sigma} \frac{e^{-\beta H[\sigma]}}{\mathcal{Z}_\beta} \left(1 - \tanh \left(\beta J \sum_{i \geq 1} \sigma_i \sigma_{\bar{i}} \right) \right) \quad (32)$$

$$= \frac{1}{2} \left[1 - \left\langle \tanh(\beta H_\partial) \right\rangle \right] \quad (33)$$

where H_∂ is the boundary Hamiltonian between A and \bar{A} .

Mapping to the $d-1$ repetition code

The problem of choosing which domain wall configuration to assume can be understood as a decoding problem for a $(d-1)$ -dimensional classical repetition code. To see this, note that the decoding task in a classical error correcting

code is basically figuring out what error has happened based on a given set of syndromes. In particular the decoding task in the classical repetition code on N bits can be described as follows. Consider an *error vector* $e \in \{1, -1\}^N$ such that $e_i = -1$ if a bit flip has happened on the i 'th bit and $e_i = 1$ otherwise. The goal of the decoder is to figure out e , knowing only the syndrome values, i.e. $e_i e_j$ for adjacent i and j on the appropriate graph, e.g. the d -dimensional square lattice in the standard d -dimensional repetition code. Moreover, the decoder assumes an underlying noise model, i.e. a random distribution from which the vector e is drawn. For example, in the independent and identically distributed (iid) noise model, it assumes each component e_i is -1 with probability p and 1 with probability $1 - p$, independent of other components.

In our setting finding the domain wall configuration is clearly the same task, with e_i defined to be $e_i \equiv \sigma_i \sigma_{\bar{i}}$. Note that we can not know the value of e_i , but we know the value of $e_i e_j = \mu_{i,j} \mu_{\bar{i},\bar{j}}$ for adjacent i and j . At low temperatures, the domain walls are rare so most e_i s would be 1 , and as one increases the temperature more e_i would be -1 . The underlying noise model is given by $P_{\mu,\tau}$ as described in the previous section. This noise model is not iid, but rather a correlated noise model. However, as we argue in the next section, the repetition code is able to guess e correctly with probability 1 in the thermodynamic limit unless $\beta = 0$, at which point each e_i is ± 1 completely at random.

Threshold for the Repetition Code

Here we argue that the repetition code decoding under the noise distribution $P_{\mu,\tau}$ is successful with probability 1 for any $\beta > 0$ in the thermodynamic limit. First we review the argument for maximum error correction threshold in the presence of the iid noise and then we argue that the same should remain true for more generic noise models. We use quantum notation for convenience although the problem we are considering is inherently classical.

Consider an initial state $|\Psi\rangle$ undergoing some errors, leaving it in the mixed state

$$\rho = \sum_e p_e e |\Psi\rangle \langle \Psi| e \quad (34)$$

where e is a product of X bit flips and p_e is the probability of having that error. We rewrite the sum to distinguish between the errors that leave ρ with fewer than $N/2$ bit flips and errors with higher weights:

$$\rho = \sum_{e:|e|<N/2} p_e e |\Psi\rangle \langle \Psi| e + \sum_{e:|e|\geq N/2} p_e e |\Psi\rangle \langle \Psi| e. \quad (35)$$

The error correction channel, \mathcal{R} , measures the syndromes, and between two possible error configuration consistent with a syndrome, applies the one with the smaller weight. Therefore it always successfully corrects the errors when there are less than $N/2$ bit flips, hence,

$$\mathcal{R}(\rho) = \sum_{e:|e|<N/2} p_e \mathcal{R}(e |\Psi\rangle \langle \Psi| e) + \sum_{e:|e|\geq N/2} p_e \mathcal{R}(e |\Psi\rangle \langle \Psi| e) \quad (36)$$

$$= \sum_{e:|e|<N/2} p_e |\Psi\rangle \langle \Psi| + \sum_{e:|e|\geq N/2} p_e \mathcal{R}(e |\Psi\rangle \langle \Psi| e). \quad (37)$$

The fidelity of this post-error correction state with the original state is lower bounded as,

$$F = \langle \Psi | \mathcal{R}(\rho) | \Psi \rangle \quad (38)$$

$$= \sum_{e:|e|<N/2} p_e + \sum_{e:|e|\geq N/2} p_e \langle \Psi | \mathcal{R}(e |\Psi\rangle \langle \Psi| e) | \Psi \rangle \geq \sum_{e:|e|<N/2} p_e \quad (39)$$

where the lower bound is because the second term in the expression above is non-negative. Now we will show that this lower bound is equal to one in the thermodynamic limit. First, we rearrange the sum to be over $|e| = k$, the number of bit flips error, and because p_k is a binomial distribution, $p_k = \binom{N}{k} p^k (1-p)^{N-k}$. In the limit of large N , we can approximate the binomial distribution as a Gaussian distribution with mean Np and standard deviation $\sqrt{Np(1-p)}$ via the central limit theorem. Since $N/2$ is $\frac{N/2 - Np}{\sqrt{Np(1-p)}} = O(\sqrt{N})$ standard deviations away from the peak of the Gaussian, we see that $\lim_{N \rightarrow \infty} \sum_{k=0}^{N/2-1} p_k = 1$ when $p < 1/2$. Since fidelity is upper-bounded by one, the fidelity is indeed equal to one in the thermodynamic limit. Thus, the repetition code will work successfully when $p < 1/2$.

For the more general case where e is drawn based on the $P_{\mu,\tau}$ distribution, the bound in Eq.(39) is still valid. Therefore, to show perfect recovery we only need to show that with probability one, less than half of the edges contain a domain wall. Intuitively, this is true because for $\beta > 0$, not having a domain wall on an edge is energetically favorable. To make it rigorous, one can define indicator variables $I_i = (1 - e_i)/2$ in terms of which the number of domain walls can be written as $k = \sum_i I_i$. When $\beta > 0$ it is more probable for I_i to be 0 rather than 1 and hence the expectation value of $k/|\partial A|$ is less than $1/2$. Noting that $\lim_{|i-j| \rightarrow \infty} \text{Cov}(I_i, I_j) = 0$, the weak law of large numbers for weakly dependent variables[56] shows that $k/|\partial A|$ concentrates around its mean, which is less than $1/2$ when $\beta > 0$ in the thermodynamic limit.

Negativity Spectrum

Here we calculate the entanglement negativity between a sub-region A and its complement \bar{A} , in the state ρ_β . Let $\bar{\sigma}$ denote the spin configuration that is related to σ by flipping every spin. Accordingly, the state $|\psi_\sigma\rangle$ can be written as $|\psi_\sigma\rangle = \frac{|\sigma\rangle + |\bar{\sigma}\rangle}{\sqrt{2}}$ and Eq. (2) can be rewritten as,

$$\rho_\beta = \frac{1}{2\mathcal{Z}_\beta} \sum_{\sigma} e^{-\beta H[\sigma]} (|\sigma\rangle \langle \sigma| + |\bar{\sigma}\rangle \langle \bar{\sigma}| + |\sigma\rangle \langle \bar{\sigma}| + |\bar{\sigma}\rangle \langle \sigma|), \quad (40)$$

where $H[\sigma] = -J \sum_{\langle i,j \rangle} \sigma_i \sigma_j$ is the classical Ising energy of the spin configuration σ . Taking the partial transpose of ρ_β with respect to sub-region A yields,

$$\begin{aligned} \rho_\beta^{T_A} &= \frac{1}{2\mathcal{Z}_\beta} \sum_{\sigma} \left[e^{-\beta H[\sigma]} (|\sigma\rangle \langle \sigma| + |\bar{\sigma}\rangle \langle \bar{\sigma}|) + e^{-\beta H[\sigma_A, \sigma_{\bar{A}}]} (|\bar{\sigma}_A, \sigma_{\bar{A}}\rangle \langle \sigma_A, \bar{\sigma}_{\bar{A}}| + |\sigma_A, \bar{\sigma}_{\bar{A}}\rangle \langle \bar{\sigma}_A, \sigma_{\bar{A}}|) \right] \\ &= \frac{1}{2\mathcal{Z}_\beta} \sum_{\sigma} \left[e^{-\beta H[\sigma]} (|\sigma\rangle \langle \sigma| + |\bar{\sigma}\rangle \langle \bar{\sigma}|) + e^{-\beta H[\sigma_A, \bar{\sigma}_{\bar{A}}]} (|\bar{\sigma}\rangle \langle \sigma| + |\sigma\rangle \langle \bar{\sigma}|) \right] \end{aligned} \quad (41)$$

where σ_A and $\sigma_{\bar{A}}$ denote the spin configuration σ restricted to regions A and \bar{A} respectively. Thus, the eigenvalues and eigenstates of $\rho_\beta^{T_A}$ are

$$\lambda_{\sigma;\pm} = \frac{e^{-\beta H[\sigma]} \pm e^{-\beta H[\sigma_A, \bar{\sigma}_{\bar{A}}]}}{\mathcal{Z}_\beta}, \quad \left| \psi_\sigma^{(\pm)} \right\rangle \equiv \frac{|\sigma\rangle \pm |\bar{\sigma}\rangle}{\sqrt{2}}. \quad (42)$$

We can now calculate the entanglement negativity from the sum of all the negative eigenvalues. Firstly, it is only the $\lambda_{\sigma;-}$ eigenvalues which can be negative. We can also see that $\lambda_{\sigma;-} = \lambda_{\bar{\sigma};-}$ from the \mathbb{Z}_2 symmetry of the Hamiltonian and they correspond to the same eigenvector, up to some phase. Moreover, note that $\lambda_{\sigma;-} = -\lambda_{\sigma_A, \bar{\sigma}_{\bar{A}};-}$ so for a given spin configuration, either $\lambda_{\sigma;-}$ or $\lambda_{\sigma_A, \bar{\sigma}_{\bar{A}};-}$ would be negative. Thus, we account for the two incidences of double counting with an additional $1/4$ and get

$$\mathcal{N}_A[\rho_\beta] = \frac{1}{4\mathcal{Z}_\beta} \sum_{\sigma} \left| e^{-\beta H[\sigma]} - e^{-\beta H[\sigma_A, \bar{\sigma}_{\bar{A}}]} \right|. \quad (43)$$

Factoring out $e^{-\beta H[\sigma]}$ we get

$$\begin{aligned} \mathcal{N}_A[\rho_\beta] &= \frac{1}{4\mathcal{Z}_\beta} \sum_{\sigma} e^{-\beta H[\sigma]} \left| 1 - e^{-\beta(H[\sigma_A, \bar{\sigma}_{\bar{A}}] - H[\sigma])} \right| \\ &= \frac{1}{4} \left\langle \left| 1 - e^{2\beta H_\partial[\sigma]} \right| \right\rangle. \end{aligned} \quad (44)$$